

Non-Newtonian fluid properties of hyperconcentrated sediment laden flow in open channel

Kumamoto University
Kumamoto University

Student member
Member

○ Liany Amelia HENDRATTA
Terunori OHMOTO

1. Introduction

Flow with high suspended sediment concentrations are common in many sedimentary environment. Such hyper-concentrated sediment laden flows have fluid-dynamics characteristics which are radically different from those of clear-water flow. As viscosity or density increases, changes are likely to occur in sediment concentration distribution, the resistance characteristics, turbulence intensity and sediment transport capacity of flow. Concerning hyper-concentrated sediment laden flow in an open channel, only a small number of studies have been conducted to obtain detailed measurement data on flow velocity changes because of the difficulty in measurement and the influence of this fluid properties on resistance and the internal flow structure remains poorly understood. Bradley and McCutcheon (1985) conducted an experiment and they pointed out that characteristics of hyper-concentrated sediment-laden flow appear at concentrations of 20% or more. Regarding the resistance characteristics of hyper-concentrated sediment-laden flows, it has been reported that resistance tended to decrease as sediment concentration increased (Wang, 1989), however, (Yang 1991) reported that resistance increased slightly at a volume concentration of clay 9%. This experimental study was conducted to investigate the resistance characteristics and the flow structures of hyper-concentrated sediment-laden flows over dune type bed through comparison with clear water flow.

2. Experimental setup and methodology

The material used for viscosity measurement are the Yellow River sediment suspensions, kaolin suspensions and sodium polyacrylate (PSA) solutions. For viscosity measurement, Brookfield's DV-II+ PRO Digital Viscometer which excels in the measurement of viscosity at low shear rates was used. Since the viscosity of non-Newtonian fluids is highly dependent on temperature, a well-insulated pipe was used to connect a constant-temperature circulating tank capable to stably keep water temperature at 20°C. An acrylic-resin circulating variable-slope flume that is 10 m long, 0.4 m wide and 0.2 m high was used in this experiment.. To simulate a continuous dune bed, 80 wavy bed segments were placed in a 6.4 meter long section from the upstream end of the flume. The origin of the coordinate system was located at the midpoint of a dune ridge 2 m downstream from the upstream end of the flume. An air-cooled double-pulse YAG laser was used as a light source for PIV and the laser light sheet was directed vertically downward from above the flume. Two images of a particle passing through the laser light sheet are captured by a CCD camera located to the side of the flume. In the PIV measurement, the flow corresponding to the

Table 1. Experimental conditions

	Clear water	PSA solution
Discharge, $Q(l/s)$	1.7	1.7
Flow depth, $H(cm)$	2.5	3.5
Mean flow velocity, $U_m(cm/s)$	17.0	12.1
Maximum flow velocity, $U_0(cm/s)$	20.8	18.0
Channel slope, i_0	1/2000	1/2000
Froude Number, Fr	0.34	0.21
Reynolds number, Re	4250	

wavelength was measured at a point 2 m downstream from the upstream end of the flume, where a flow field in a state of equilibrium was formed. Table 1 shows the experiment conditions. In the experiment conducted by using a PSA solution with viscosity characteristics similar to those of hyperconcentrated sediment-laden flow, the slope of the flume, the flow rate and the bed boundary conditions of the hyperconcentrated sediment-laden flow were made identical to those of clear water flow. The water depth difference between the clear water and the PSA solution shown in the table is due to the differences in resistance characteristics.

3. Experimental results

Figure 1 shows changes in the average water depth h_m corresponding to the unit width flow rate q in the clear water and PSA solution cases. On the whole, the ranging from 1.06 to 1.13 times as large. Figure 2 shows the relationship between the total resistance coefficient C_f and the unit width flow rate. The ratio of the total resistance coefficient of the PSA solution to that of clear water, $C_{f_{psa}}/C_{f_w}$, tended to decrease as the unit width flow rate increased and ranged from 1.22 to 1.46.

Figure 3 shows how the vertical distribution of main flow velocity changes in the flow direction over a dune-type bed in the clear water case and the PSA solution case. The vertical distribution of main flow velocity shows characteristics of a free mixing layer behind a ridge, suggesting the growth of an internal boundary layer along the bed surface further downstream and the influence of flow acceleration due to the forward pressure gradient. In the PSA solution case, unlike in the clear water case, there are two clearly-discernible high-shear-rate areas. The solid line in the clear water case indicates the flow separation line. It can also be seen that flow separation and the resultant development of circulation flows are not pronounced in the PSA solution case.

Figures 4 show how the vertical distribution of turbulence intensity in the streamwise direction changes in the flow direction.

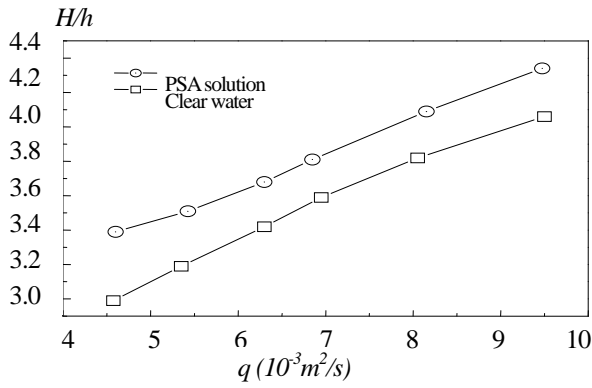


Fig. 1. Relationship between uniform flow depth and unit width flow rate

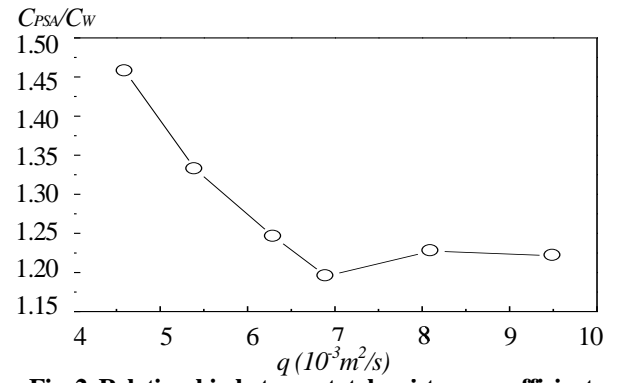


Fig. 2. Relationship between total resistance coefficient and unit width flow rate

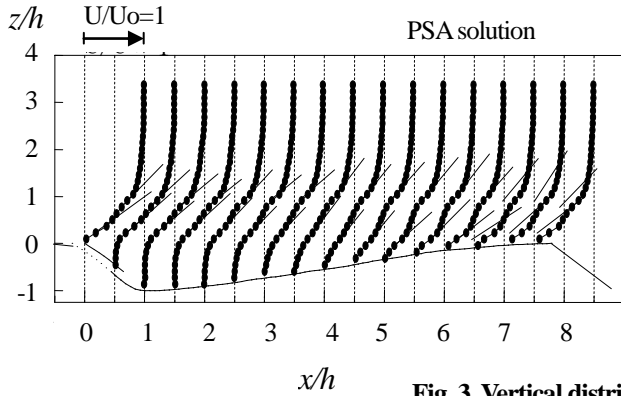


Fig. 3. Vertical distribution of main flow velocity

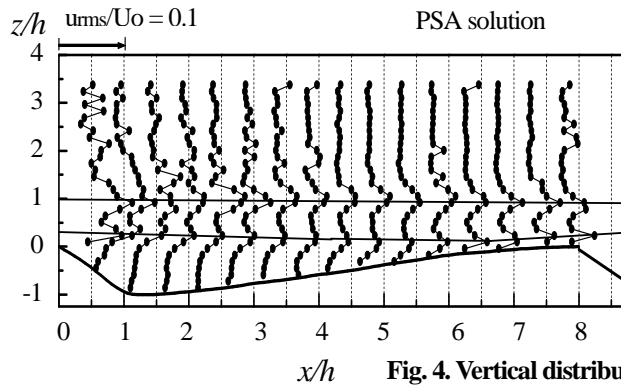
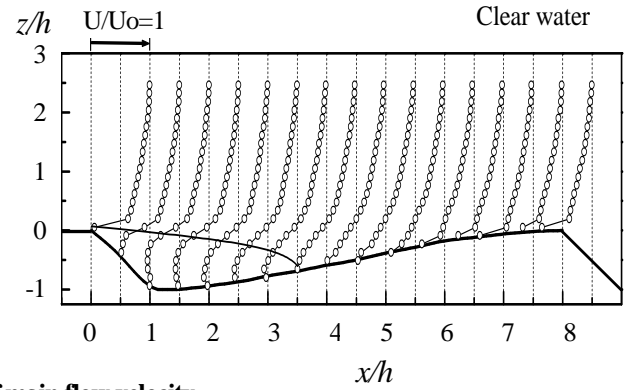
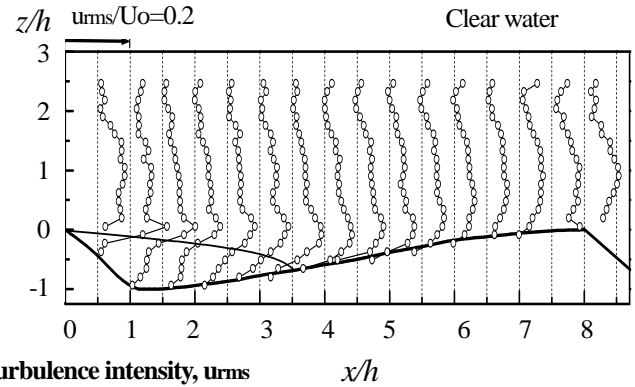


Fig. 4. Vertical distribution of turbulence intensity, u_{rms}



The solid lines in the figures were drawn to connect the maximum values of turbulence intensity at different flow distances. In the PSA solution case, the maximum values of turbulence intensity at two height levels, namely, $z/h = 1$ and $z/h = 0.2$ to 0.3 , both in the streamwise direction and in the vertical direction. In the clear water case, turbulence intensity tended to increase in the deceleration region from the upstream ridge to the reattachment point and decreased considerably near the bed surface in the acceleration region from $z/h = 4$ to the downstream ridge. Compared with the clear water case, in the high-viscosity PSA solution case, turbulence intensity decreased to about 50% in the streamwise direction and about 30% in the vertical direction. In the vertical distribution of turbulence intensity in the PSA solution case, the maximum values occurred at two locations under the influence of flow separation and shear deformation of the internal boundary layer of the bed. This greatly differs from what was observed in the clear water case.

4. Conclusion

The total resistance coefficient of PSA solution was greater than clear water by a factor of up to 1.46. In the PSA solution, flow separation and the resultant development of circulating flow were not conspicuous, and a region with a high shear rate was seen at $z/h = 1$ and $z/h = 0.2-0.3$. Turbulence intensities were about 50% in the streamwise direction and about 30% in the vertical direction of those in the clear water. The location of the maximum value of turbulence intensity in the PSA solution showed close agreement with the location of the maximum value of the shear rate.

References

- Wang H., and X. Fei, "The fluctuation of Bingham shear stress on hyperconcentrated flow in flowing conditions", *Proceeding of 4th Intern. Symp. on River Sedimentation*, (1989), pp.198-205
- Yang, C.T., and X. Kong, "Energy Dissipation Rate and Sediment Transport", *Journal of Hydraulic Research*, Vol.29, No.4, (1991).